View metadata, citation and similar papers at core.ac.uk
brought to you by CORE
provided by ELTE Digital Institutional Repository (EDIT)

Draft version September 10, 2018
Preprint typeset using LaTeX style emulateapj v. 08/22/09

arXiv:0809.4295v2 [astro-ph] 8 Oct 2008

HAT-P-10b: A LIGHT AND MODERATELY HOT JUPITER TRANSITING A K DWARF†

G. Á. Bakos[1,2], A. Pál[1,4], G. Torres[1], B. Sipőcz[1,4], D. W. Latham[1], R. W. Noyes[1], Géza Kovács[3], J. Hartman[1], G. A. Esquerdo[1], D. A. Fischer[6], J. A. Johnson[7], G. W. Marcy[5], R. P. Butler[8], A. Howard[5], D. D. Sasselov[1], Gábor Kovács[1], R. P. Stefanik[1], J. Lázár[9], I. Papp[9], P. Sári[9]

Draft version September 10, 2018

ABSTRACT

We report on the discovery of HAT-P-10b, the lowest mass ($0.46 \pm 0.03\,M_{\rm J}$) transiting extrasolar planet (TEP) discovered to date by transit searches. HAT-P-10b orbits the moderately bright V=11.89 K dwarf GSC 02340-01714, with a period $P = 3.7224690 \pm 0.0000067\,d$, transit epoch $T_c = 2454729.90631 \pm 0.00030$ (BJD) and duration 0.1100 ± 0.0015 d. HAT-P-10b has a radius of $1.05^{+0.05}_{-0.03}\,R_{\rm J}$ yielding a mean density of $0.498 \pm 0.064\,{\rm g\,cm^{-3}}$. Comparing these observations with recent theoretical models we find that HAT-P-10 is consistent with a ~ 4.5 Gyr, coreless, pure hydrogen and helium gas giant planet. With an equilibrium temperature of $T_{eq} = 1030^{+26}_{-19}\,K$, HAT-P-10b is one of the coldest TEPs. Curiously, its Safronov number $\theta = 0.047 \pm 0.003$ falls close to the dividing line between the two suggested TEP populations.

Subject headings: planetary systems — stars: individual (HAT-P-10, GSC 02340-01714) techniques: spectroscopic, photometric

1. INTRODUCTION

It has become clear in recent years that transiting extrasolar planets (TEPs), especially those around bright stars, are extremely valuable for understanding the physical properties of planetary bodies. The transit itself is a periodic event, which — together with high precision spectroscopic observations and radial velocity (RV) follow-up – reveals a number of key parameters, notably the relative radius of the planet with respect to the star, and the true mass of the planet without the inclination ambiguity. These allow determination of the mean density of the planet, and an insight into its basic structural properties. These advantages have been realized early on, and the recent rise in the detection of TEPs is due to a number of dedicated transit searches, such as TrES (Brown & Charbonneau 2000; Dunham et al. 2004), XO (McCullough et al. 2005), SuperWASP (Pollacco et al. 2006), OGLE (targeting fainter stars; Udalski et al. 2008), and HATNet (Bakos et al. 2002, 2004). At the time of this writing, the number of published TEPs with a unique identification is $\sim$ 40, with $\sim$ 35 of these due to systematic searches. The properties of known TEPs already span a wide range, from the hot Neptune GJ436b with a mass of $M_p = 0.072\,M_{\rm J}$ (Butler et al. 2004; Gillon et al. 2007) to XO-3 with $M_p = 11.79 M_p$ (Johns-Krull et al. 2008), from short period orbits like OGLE-TR-56b with $P = 1.2$ days (Udalski et al. 2002; Konacki et al. 2003) to $P = 21.2$ days of HD 17506b (Barbieri et al. 2007). Although most of these planets have circular orbits, some planets with significant eccentricities, such as HAT-P-2b (Bakos et al. 2007a), have also been reported. TEPs have been discovered in a wide range of environments, from orbiting M dwarfs (GJ436b) up to mid F-dwarfs, such as HAT-P-7b (Pál et al. 2008a).

Theoretical investigations have been thriving during this vigorous discovery era, some focusing on the radius of these planets (Burrows et al. 2007; Liu et al. 2008; Chabrier et al. 2004; Fortney et al. 2007), and others on the atmospheres (e.g. Burrows et al. 2006; Fortney et al. 2007), to mention two of the key observable properties of transiting planets. When confronting theory with observations, it is also essential to use accurate observational values, along with proper error estimates. The recent compilation of TEP parameters by Torres, Winn & Holman (2008) represents a step forward in this sense. It was also noted throughout these works that a much larger sample is required for better understanding of the underlying physics, i.e. more planets are needed to populate the mass–radius (or other) parameter space, to improve the statistical significance of correlations between planetary and stellar parameters, and to reveal any previously undetected correlations that may shed light on the physical processes governing the formation and evolution of TEPs.

The HATNet survey has been a major contributor to TEP discoveries. Operational since 2003, it has covered approximately 7% of the Northern sky, searching for TEPs around bright stars ($8 \lesssim I \lesssim 12$ mag). HATNet operates six wide field instruments: four at the Fred Lawrence Whipple Observatory (FLWO) in Arizona, and two on the roof of the Submillimeter Array

[1] Harvard-Smithsonian Center for Astrophysics, Cambridge, MA, gbakos@cfa.harvard.edu
[2] NSF Fellow
[3] Konkoly Observatory, Budapest, Hungary
[4] Department of Astronomy, Eötvös Loránd University, Budapest, Hungary.
[5] Department of Astronomy, University of California, Berkeley, CA
[6] Department of Physics and Astronomy, San Francisco State University, San Francisco, CA
[7] Institute for Astronomy, University of Hawaii, Honolulu, HI 96822; NSF Postdoctoral Fellow
[8] Department of Terrestrial Magnetism, Carnegie Institute of Washington, DC
[9] Hungarian Astronomical Association, Budapest, Hungary

† Based in part on observations obtained at the W. M. Keck Observatory, which is operated by the University of California and the California Institute of Technology. Keck time has been granted by NOAO (A285Hr) and NASA (N128Hr).

Hangar (SMA) of SAO. Since 2006, HATNet has announced and published 9 TEPs. In this work we report on the tenth such discovery.[11].

2. PHOTOMETRIC DETECTION

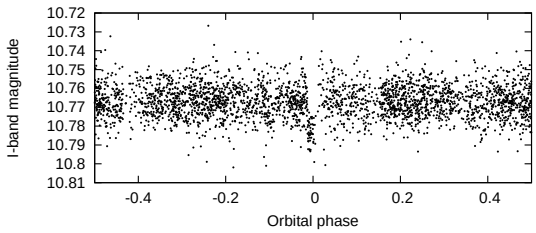

FIG. 1.— The unbinned light curve of HAT-P-10 including all 2870 instrumental I-band measurements obtained with the HAT-10 telescope of HATNet (see text for details), and folded with the period of $P = 3.7224690$ days (which is the result the fit described in § 4).

The transits of HAT-P-10b were detected with one of the HATNet telescopes, HAT-10, located at FLWO. The region around GSC 02340-01714, a field internally labeled as G213, was observed on a nightly basis between 2005 October 3 and 2006 March 14, whenever weather conditions permitted. We gathered 2870 exposures of 5 minutes at a 5.5-minute cadence. Each image contained approximately 29,000 stars down to $I \sim 14.0$. For the brightest stars in the field we achieved a per-image photometric precision of 4 mmag.

The calibration of the HATNet frames was done utilizing standard procedures. The calibrated frames were then subject to star detection and astrometry, as described in Pál & Bakos (2006). Aperture photometry was performed on each image at the stellar centroids derived from the 2MASS catalog (Cutri et al. 2003) and the individual astrometrical solutions. The resulting light curves were decorrelated against trends using the External Parameter Decorrelation technique (EPD, see Bakos et al. 2007b) and the Trend Filtering Algorithm (TFA, see Kovács et al. 2005). The light curves were searched for periodic box-like signals using the Box Least Squares method (BLS, see Kovács et al. 2002). We detected a significant signal in the light curve of GSC 02340-01714 (also known as 2MASS 03092855+3040249; $\alpha = 03^{\rm h}09^{\rm m}28.55^{\rm s}$, $\delta = +30^{\rm d}40^{\rm m}24.9^{\rm s}$; J2000), with a depth of ~ 15 mmag, and a period of $P = 3.7225$ days. The dip had a relative duration (first to last contact) of $q \approx 0.027$, equivalent to a total duration of $Pq \approx 2.5$ hours (see Fig. 1).

3. FOLLOW-UP OBSERVATIONS

3.1. *Reconnaissance Spectroscopy*

All HATNet candidates are subject to thorough investigation before using more precious time on large telescopes, such as Keck I, to observe them. One of the important tools for establishing whether the transit-feature in the light curve of a candidate is due to astrophysical phenomena other than a planet transiting a star is the CfA Digital Speedometer (DS; Latham 1992), mounted on the FLWO 1.5 m telescope.

[11] After submission of this paper, it was realized that HAT-P-10b and WASP-11b refer to the same object, independently discovered, with WASP-11b submitted 7 days earlier to A&A. The two discovery groups agreed on calling it in future papers as WASP-11b/HAT-P-10b, with separate entries on www.exoplanet.eu

TABLE 1
RELATIVE RADIAL VELOCITY MEASUREMENTS OF HAT-P-10

BJD (2,454,000+)	RV ($\rm m\,s^{-1}$)	$\sigma_{\rm RV}$ ($\rm m\,s^{-1}$)
547.76983	−0.9	3.7
548.75614	−18.8	1.8
675.11598	−27.8	1.8
723.07574	−25.8	1.5
725.08480	103.0	2.0
727.13146	−37.4	1.8

High-resolution spectra with low signal-to-noise ratio from this facility have been used routinely in the past to derive radial velocities with moderate precision (roughly $1\,\rm km\,s^{-1}$) and to classify the effective temperature and surface gravity of the host star, to weed out false alarms, such as F dwarfs orbited by M dwarfs, grazing eclipsing binaries, triple and quadruple star systems, or giant stars where the transit signal is either false, or comes from a nearby, blended eclipsing binary.

The RV measurements of HAT-P-10 showed an rms residual of $0.43\,\rm km\,s^{-1}$, consistent with no detectable RV variation. Atmospheric parameters for the star, including the effective temperature $T_{\rm eff} = 5000\,K$, surface gravity $\log g = 4.5$, and projected rotational velocity $v \sin i = 1.5 \rm km\,s^{-1}$, were derived as described by Torres et al. (2002). The effective temperature and surface gravity corresponds to an early K dwarf.

3.2. *High resolution, high S/N spectroscopy*

Given the significant detection by HATNet, and the positive DS results that exclude the usual suspects, we proceeded with the follow-up of this candidate by obtaining high-resolution and high S/N spectra to characterize the radial velocity variations and to determine the stellar parameters with higher precision. We obtained 6 exposures with an iodine cell, plus one iodine-free template, using the HIRES instrument (Vogt et al. 1994) on the Keck I telescope located on Mauna Kea, Hawaii. The observations were made on the nights of 2008 March 21-22, July 27 and on three nights between September 13 and 17. The small RV variations based on the March 2007 run made this target a firm planet candidate, but more observations were required to derive an orbit, and to check spectral bisector variations (see § 4.2).

The width of the spectrometer slit used on HIRES was $0\farcs86$, resulting in a resolving power of $\lambda/\Delta\lambda \approx 55{,}000$, with a wavelength coverage of $\sim 3800 - 8000$ Å. The iodine gas absorption cell was used to superimpose a dense forest of I_2 lines on the stellar spectrum and establish an accurate wavelength fiducial (see Marcy & Butler 1992). Relative RVs in the Solar System barycentric frame were derived as described by Butler et al. (1996), incorporating full modeling of the spatial and temporal variations of the instrumental profile. The final RV data and their errors are listed in Table 1. The folded data, with our best fit (see § 4) superimposed, are plotted in Fig. 2.

3.3. *Photometric follow-up observations*

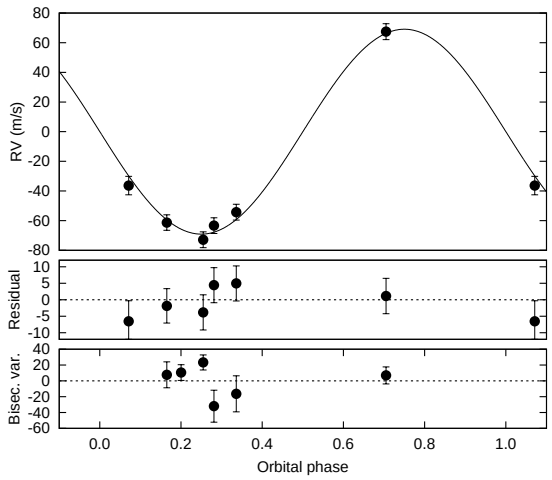

FIG. 2.— (Top) Radial-velocity measurements from Keck for HAT-P-10, along with an orbital fit, shown as a function of orbital phase, using our best fit period (see § 4). The center-of-mass velocity has been subtracted. (Middle) Phased residuals after subtracting the orbital fit (also see § 4). The rms variation of the residuals is about $4.2\,\mathrm{m\,s^{-1}}$. (Bottom) Bisector spans (BS) for 5 of the 6 Keck spectra plus the single template spectrum (§ 4.2). The mean value has been subtracted. Note the different vertical scale of the panels.

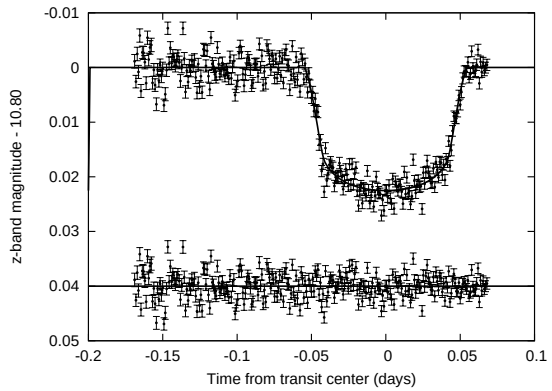

FIG. 3.— Unbinned instrumental Sloan z-band transit light curve acquired with KeplerCam at the FLWO 1.2 m telescope on 2008 September 19 MST; superimposed is the best-fit transit model light curve. Below we show the residuals from the fit.

We observed a complete transit event of HAT-P-10 on the night of 2008 September 19/20 MST with the KeplerCam CCD on the FLWO 1.2 m telescope. Altogether 278 frames were acquired with a cadence of 65 seconds in Sloan z band. The reduction of the images was performed as follows. After bias and flat calibration, we derived an initial second order astrometrical transformation between the ~ 110 brightest stars and the 2MASS catalog, as described in Pál & Bakos (2006), yielding a residual of ~ 0.3 pixels. In order to avoid systematic errors resulting from the proper motion of the stars, we generated a new catalog. This catalog was based on the detected stellar centroids, the coordinates of which were transformed to the same reference system using the initial astrometrical solutions, and then averaged out using 3-σ rejection. Using this new catalogue as reference, the final astrometrical solution was derived for each frame, yielding a residual of ~ 0.04 pixel. In the next step, aperture photometry was performed using a series of apertures with radii of 6.0, 7.5, 9.0 and 10.5 pixels. The instrumental magnitude transformation was also done in two steps: first, all magnitude values were transformed to the photometric reference frame (selected to be the sharpest image), using the individual Poisson noise error estimations as weights. In the second step, the magnitude fit was repeated using the mean individual light curve magnitudes as reference and the rms of these light curves as weights. In both of the magnitude transformations, we excluded from the fit the target star itself and the 3-σ outliers. We performed EPD against trends simultaneously with the light curve modeling (for more details, see § 4). From the series of apertures we chose the one with a radius of 9.0 pixels, yielding the smallest fit rms. This aperture falls in the middle of the aperture series, confirming the plausible selection for the apertures. The final light curve is shown in the upper plot of Fig. 3, superimposed with our best fit transit light curve model (see also § 4).

4. ANALYSIS

In this section we describe briefly our analysis yielding the orbital, planetary and stellar parameters of the HAT-P-10 system.

4.1. *Planetary, orbital and stellar parameters*

First, using the template spectrum obtained by the Keck/HIRES instrument, we derived the stellar atmospheric parameters. We used the SME package of Valenti & Piskunov (1996), which yielded the following values with conservative errors: $T_{\rm eff} = 4980 \pm 60\,\mathrm{K}$, $\log g_\star = 4.5 \pm 0.1\,(\mathrm{cgs})$, [Fe/H] $= 0.13 \pm 0.08$, and $v \sin i = 0.5 \pm 0.2\,\mathrm{km\,s^{-1}}$.

In modeling both the HATNet and the follow-up transit light curves, we used the quadratic limb darkening formalism of Mandel & Agol (2002). The limb darkening coefficients used for the above stellar atmospheric parameters by interpolating in the tables provided by Claret (2004). The coefficients we derived for I and z photometric passbands were $\gamma_{1(I)} = 0.3806$, $\gamma_{2(I)} = 0.2535$, $\gamma_{1(z)} = 0.3214$, and $\gamma_{2(z)} = 0.2693$.

Following this, a joint fit was done using all of the available data, including the HATNet light curve, the follow-up light curve and the radial velocity measurements. Throughout the analysis, we refer to the transit event observed on 2008 September 19/20 as $N_{\rm tr} = 0$.

We adjusted the following parameters: $T_{\rm c,-290}$, the time of first transit center in the HATNet campaign; $T_{\rm c,0}$, the time of the transit center on September 19/20; K, the radial velocity semi-amplitude; $k = e\cos\omega$ and $h = e\sin\omega$, the Lagrangian orbital elements related to the eccentricity and argument of periastron; $p \equiv R_{\rm p}/R_\star$, the fractional planetary radius; b^2, the square of the impact parameter; the quantity $\zeta/R_\star$, which is related to the transit duration $T_{\rm dur}$ as $(\zeta/R_\star)^{-1} = T_{\rm dur}/2$; and M_0 and M_1, the out-of-transit instrumental magnitudes of the HATNet and FLWO/KeplerCam light curves. As noted by Bakos et al. (2007b), the quantity $\zeta/R_\star$ shows only a small correlation with the other light curve parameters ($R_{\rm p}/R_\star$, b^2), which makes it a good parameter to use. For eccentric orbits, this quantity is related to the normalized semi-major axis $a/R_\star$ as $\zeta/R_\star = (2\pi/P)(a/R_\star)\sqrt{1-e^2}(1-b^2)^{-1/2}(1+h)^{-1}$. To

TABLE 2
Stellar parameters for HAT-P-10

Parameter	Value	Source
$T_{\rm eff}$ (K)	4980 ± 60	SME[a]
[Fe/H]	0.13 ± 0.08	SME
$v \sin i$ (km s^{-1})	0.5 ± 0.2	SME
$M_\star$ ($M_\odot$)	0.82 ± 0.03	Y^2+LC+SME[b]
$R_\star$ ($R_\odot$)	$0.81^{+0.03}_{-0.02}$	Y^2+LC+SME
$\log g_\star$ (cgs)	4.54 ± 0.03	Y^2+LC+SME
$L_\star$ ($L_\odot$)	$0.36^{+0.04}_{-0.03}$	Y^2+LC+SME
M_V (mag)	6.12 ± 0.12	Y^2+LC+SME
Age (Gyr)	11.2 ± 4.1	Y^2+LC+SME
Distance (pc)	125^{+6}_{-5}	Y^2+LC+SME

[a] SME = 'Spectroscopy Made Easy' package for analysis of high-resolution spectra Valenti & Piskunov (1996). See text.
[b] Y^2+LC+SME = Yale-Yonsei isochrones (Yi et al. 2001), light curve parameters, and SME results.

find the best fit values and the uncertainties, we utilized the method of Markov Chain Monte-Carlo (MCMC; Ford 2006) which provides the *a posteriori* distribution of the adjusted parameters.

The values and uncertainties of the k and h orbital elements were found to be consistent with zero within 1-σ, namely $k = 0.04 \pm 0.11$ and $h = 0.11 \pm 0.12$. Therefore we conclude that the observations are consistent with a circular planetary orbit, and we repeated the fit by fixing the eccentricity to zero.

The results for the simultaneous fit are reported in Table 3, except for the auxiliary parameters $T_{\rm c,-290} = 2453650.39029 \pm 0.00195$ (BJD), $T_{\rm c,0} = 2454729.90631 \pm 0.00030$ (BJD) that are used to derive the epoch and the period as shown in Pál et al. (2008a). The RV jitter is the additional velocity uncertainty that should be added quadratically to the nominal errors (estimated from the Poisson-noise) in order to have a reduced χ^2 of unity (this is the quadratic sum of the residuals, divided by the degrees of freedom of the RV fit, i.e. 4). Our final value for the jitter is $4.2\,{\rm m\,s^{-1}}$, and the error-bars on Fig. 2 (top and middle panel) have been inflated accordingly.

The results of the joint fit, together with the initial results from spectroscopy enable us to refine the parameters of the star. As described by Sozzetti et al. (2007) and Torres, Winn & Holman (2008), $a/R_\star$ is a better luminosity indicator than the spectroscopic value of $\log g_\star$ since stellar surface gravity has only a subtle effect on the line profiles. Therefore, we used the values of $T_{\rm eff}$ and [Fe/H] from the initial SME analysis, together with the distribution of $a/R_\star$ to estimate the stellar properties from comparison with the Yonsei-Yale (Y^2) stellar evolution models by Yi et al. (2001) and Demarque et al. (2004). Using the relation between $a/R_\star$ and $\zeta/R_\star$, we derive the *a posteriori* distribution for the former one, and used the derived stellar density as an input for the stellar evolution models in order to have an *a posteriori* distribution for the stellar parameters (see Pál et al. 2008a,c, for more details). Since the mass and radius (and their respective distributions) of the star are known, it is straightforward to obtain the surface gravity and its uncertainty together. The derived surface gravity is $\log g_\star = 4.54 \pm 0.03$. Since the surface gravity from the initial SME analysis agrees well with the one derived above, we accept the latter as final value (listed, together with other parameters in Table 2).

TABLE 3
Orbital and planetary parameters

Parameter	Value
Light curve parameters	
P (days)	3.7224690 ± 0.0000067
E (BJD)	$2454729.90631 \pm 0.00030$
T_{14} (days) [a]	0.1100 ± 0.0015
$T_{12} = T_{34}$ (days) [a]	0.0136 ± 0.0014
b^2	0.092 ± 0.062
$\zeta/R_\star\,{\rm day}^{-1}$	20.72 ± 0.14
$a/R_\star$	$11.93^{+0.21}_{-0.57}$
$R_p/R_\star$	0.1332 ± 0.0013
$b \equiv a\cos i/R_\star$	$0.238^{+0.130}_{-0.093}$
i (deg)	88.5 ± 0.6
Spectroscopic parameters	
K (m s^{-1})	69.1 ± 3.5
γ (km s^{-1})	35.5 ± 3.0
e	0 (adopted)
Planetary parameters	
M_p ($M_{\rm J}$)	0.460 ± 0.028
R_p ($R_{\rm J}$)	$1.045^{+0.050}_{-0.033}$
$C(M_p, R_p)$	0.025
ρ_p (g cm^{-3})	0.498 ± 0.064
a (AU)	$0.0439^{+0.0006}_{-0.0009}$
$\log g_p$ (cgs)	$3.02^{+0.04}_{-0.05}$
$T_{\rm eq}$ (K)	1030^{+26}_{-19}
Θ	0.047 ± 0.003

[a] T_{14}: total transit duration, time between first and last contact; $T_{12} = T_{34}$: ingress/egress time, time between first and second, or third and fourth contact.

The stellar evolution modeling also yields the absolute magnitudes and colors in various photometric passbands. The derived $V - I$ color of the star is $(V - I)_{\rm YY} = 0.917 \pm 0.019$, slightly smaller than the color from the TASS catalog (Droege et al. 2006), namely $(V-I)_{\rm TASS} = 1.09 \pm 0.11$. Since this excess is most likely due to interstellar reddening, we used the 2MASS J magnitude to estimate the distance. The observed J band magnitude of HAT-P-10 is $J = 10.015 \pm 0.020$ while the stellar modeling gives $M_J = 4.530 \pm 0.087$, which lead to a distance modulus for the star of $J - M_J = 5.484 \pm 0.089$, corresponding to a distance of $d = 125^{+6}_{-5}$ pc.

The planetary parameters and their uncertainties can be derived by direct combination of the *a posteriori* distributions of the light curve, radial velocity and stellar parameters (see also Pál et al. 2008a). We find that the mass of the planet is $M_p = 0.460 \pm 0.028\,M_{\rm J}$, the radius is $R_p = 1.045^{+0.050}_{-0.033}\,R_{\rm J}$, and its density is $\rho_p = 0.498 \pm 0.064\,{\rm g\,cm^{-3}}$. The final planetary parameters are summarized at the bottom of Table 3.

4.2. *Excluding blend scenarios*

Following Torres et al. (2007), we explored the possibility that the measured radial velocities are not real, but are instead caused by distortions in the spectral line profiles due to contamination from a nearby unresolved eclipsing binary. A bisector analysis based on the Keck spectra was done as described in earlier HATNet detection papers (see §5 in Bakos et al. (2007a)).

The first spectrum in Table 1 is contaminated, as it was

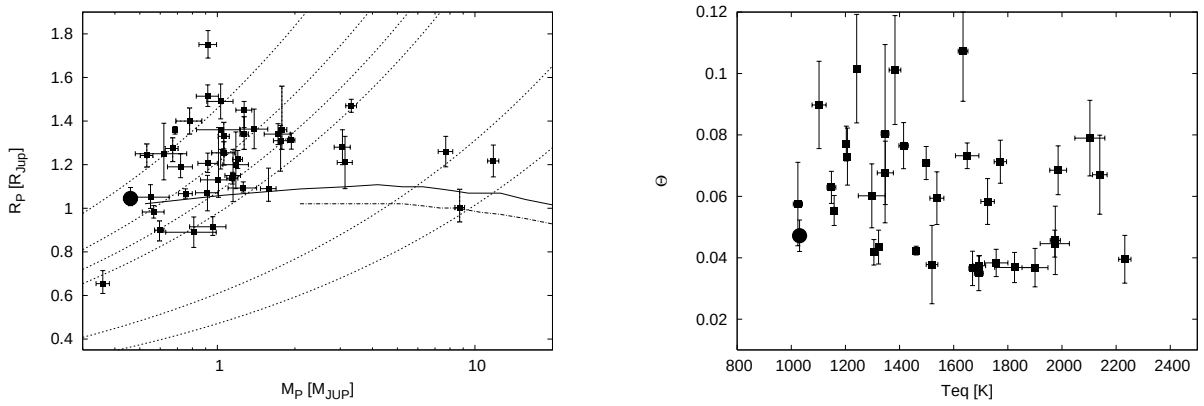

FIG. 4.— (Left): Mass–radius diagram of published and uniquely identified TEPs. HAT-P-10b is shown as a large filled circle on the left. Overlaid are Baraffe et al. (2003) zero insolation planetary isochrones for ages of 0.5 Gyr (upper, solid line) and 5 Gyr (lower dashed-dotted line), respectively, as well as isodensity lines for 0.4, 0.7, 1.0, 1.33, 5.5 and 11.9g cm^{-3}(dashed lines). (Right): Equilibrium temperature versus Safronov number (Hansen & Barman 2007).

taken at high airmass, through cloud-cover and in strong moon-light. While the RV does not seem to be affected, the bisector span is unreliable, thus we omitted it from the analysis. We detect no bisector variation in excess of the measurement uncertainties (see Fig. 2 bottom panel). We have also tested the significance of the correlation between the radial velocity and the bisector variations, and these appear to be negligible. Therefore, we conclude that the velocity variations are real, and that the star is orbited by a close-in giant planet.

5. DISCUSSION

It is interesting to compare the properties of HAT-P-10b with the other known TEPs so as to place it in a broader context. This planet falls at the low-mass end of the current distribution, as shown in Fig. 4 (left panel), where we overplot Baraffe et al. (2003) planetary isochrones, which indicate that the radius of HAT-P-10 is broadly consistent with these models. As we noted earlier, HAT-P-10 is formally the smallest mass TEP discovered by transit searches. The even smaller HD 149026b (Sato et al. 2005) and GJ436b (Butler et al. 2004) were discovered by RV searches, and their transits were found later.

We compared our mass and radius to theoretical estimates of Liu et al. (2008) for a $0.5\,M_{\rm J}$ body at various orbital distances from a G2V star. We note that the equivalent semi-major axis (with the same incident flux) of HAT-P-10b around a solar type star is $a_{rel} = 0.076$. It is also noteworthy that when a detailed comparison is done, the effects of the environment on the planetary properties are not as simple as scaling the integrated stellar flux, since the detailed spectrum of the star (e.g. UV flux) may also be important.

Based on the models presented by Liu et al. (2008), for $\dot{E}_h/\dot{E}_{ins} = 10^{-6}$ the equilibrium radius of HAT-P-10b would be $\sim$1.1 $R_{\rm J}$, where $\dot{E}_h$ is the energy per unit time due to orbital tidal heating or similar internal heating, and $\dot{E}_{ins}$ is the energy received via insolation. For larger values of $\dot{E}_h/\dot{E}_{ins}$ the expected radius is larger, and for smaller values it asympotically converges to 1.1 $R_{\rm J}$. This makes us conclude that a small core of approx. $20 M_\oplus$ is required so that the model values match the observed $1.05\,R_{\rm J}$ radius of HAT-P-10b. This would be also consistent with the core-mass—stellar metallicity relation proposed by Burrows et al. (2007)

When comparing with models of Fortney et al. (2008), we obtain similar results. The current mass, radius and insolation of HAT-P-10b are consistent with a 500 Myr model with a $25\,M_\oplus$ core mass, or a 4.5 Gyr coreless pure hydrogen and helium model. It is noted that low-mass, core-free planets are hard to model, thus our current finding will hopefully provide a further constraint for theoretical models.

The radiation that HAT-P-10b receives from its host star is $\sim 2.56 \cdot 10^8$erg s^{-1} cm^{-2}. With the definitions of Fortney et al. (2008), HAT-P-10b belongs to the pL class of planets. There is only one transiting planet that has a lower mean incident flux: HD 17156b (Barbieri et al. 2007), but this planet orbits on a highly eccentric orbit, with incident flux increasing to over 10^9erg s^{-1} cm^{-2} at periastron.

The other planet with a similarly low incident flux is OGLE-TR-111b (Udalski et al. 2002; Pont et al. 2004), orbiting an $I = 15.55$ mag star with $T_{\rm eff} = 5040\,K$ (Santos, 2006). HAT-P-10b appears to be a near-by analog of OGLE-TR-111b in many respects, since their parameters are very similar (parentheses show those of OGLE-TR-111); the period is 3.7225 d (4.01 d), the stellar mass is $0.82\,M_\odot$ ($0.85\,M_\odot$), the stellar radius is $0.81 (0.83\,R_\odot)$, the luminosity is 0.36 (0.4), the metallicity is 0.13 ± 0.08 (0.19 ± 0.07), and the planetary radius is $1.05\,M_{\rm J}$ (1.05). Interestingly, even the impact parameter of their transits is similar. There is a slight difference in their masses, with HAT-P-10b being smaller ($0.46 \pm 0.03\,M_{\rm J}$ vs. $0.55 \pm 0.1 M_{\rm J}$). One crucial difference between the two systems is that HAT-P-10 is 10 times closer to us, being at 125^{+6}_{-5} pc vs. 1500 pc for OGLE-TR-111, and is more than 4 magnitudes brighter, thus enabling more detailed follow-up in the near future.

Another interesting observational fact is that the $\Theta = 0.047 \pm 0.003$ Safronov number of HAT-P-10b falls fairly close to the dividing line between the proposed Class I and Class II planets (Hansen & Barman 2007). At the low end of the equilibrium temperature range of the plot (excluding GJ436b), HAT-P-10b seems to be at a point where the two distributions overlap (see Fig. 4, right panel). Finally, we note that HAT-P-10b strengthens the orbital period vs. surface gravity rela-

tion (Southworth, Wheatley, & Sams 2007), falling almost exactly on the linear fit between these two quantities (Torres, Winn & Holman 2008).

HATNet operations have been funded by NASA grants NNG04GN74G, NNX08AF23G and SAO IR&D grants. Work of G.Á.B. and J. Johnson were supported by the Postdoctoral Fellowship of the NSF Astronomy and Astrophysics Program (AST-0702843 and AST-0702821, respectively). We acknowledge partial support also from the Kepler Mission under NASA Cooperative Agreement NCC2-1390 (D.W.L., PI). G.K. thanks the Hungarian Scientific Research Foundation (OTKA) for support through grant K-60750. This research has made use of Keck telescope time granted through NOAO (program A285Hr) and NASA (N128Hr).

REFERENCES

Bakos, G. Á., Lázár, J., Papp, I., Sári, P. & Green, E. M. 2002, PASP, 114, 974
Bakos, G. Á., Noyes, R. W., Kovács, G., Stanek, K. Z., Sasselov, D. D., & Domsa, I. 2004, PASP, 116, 266
Bakos, G. Á., et al. 2007a, ApJ, 670, 826
Bakos, G. Á., et al. 2007b, ApJ, 671, L173
Baraffe, I., Chabrier, G., Barman, T. S., Allard, F., & Hauschildt, P. H. 2003, A&A, 402, 701
Barbieri, M., et al. 2007, A&A, 476, L13
Brown T. M. & Charbonneau D. 2000, In *Disks, Planetesimals, and Planets* (F. Garzón et al., eds.), pp. 584-589. ASP Conf. Series, San Francisco.
Burrows, A., Sudarsky, D., and Hubeny, I. 2006, ApJ, 650, 1140
Burrows, A., Hubeny, I., Budaj, J., & Hubbard, W. B. 2007, ApJ, 661, 502
Butler, R. P. et al. 1996, PASP, 108, 500
Butler, R. P., Vogt, S. S., Marcy, G. W., Fischer, D. A., Wright, J. T., Henry, G. W., Laughlin, G., & Lissauer, J. J. 2004, ApJ, 617, 580
Chabrier, G., Barman, T., Baraffe, I., Allard, F., & Hauschildt, P. H. 2004, ApJ, 603, L53
Claret, A. 2004, A&A, 428, 1001
Cutri, R. M., et al. 2003, The IRSA 2MASS All-Sky Point Source Catalog, NASA/IPAC Infrared Science Archive
Demarque et al. 2004, ApJ, 155, 667
Droege, T. F., Richmond, M. W., & Sallman, M. 2006, PASP, 118, 1666
Dunham, E. W., Mandushev, G. I., Taylor, B. W., & Oetiker, B. 2004, PASP, 116, 1072
Ford, E. 2006, ApJ, 642, 505
Fortney, J. J., Lodders, K., Marley, M. S., & Freedman, R. S. 2008, ApJ, 678, 1419
Fortney, J. J., Marley, M. S., & Barnes, J. W. 2007, ApJ, 659, 1661
Gillon, M., et al. 2007, A&A, 472, L13
Hansen, B. M. S., & Barman, T. 2007, ApJ, 671, 861
Konacki, M., Torres, G., Jha, S., & Sasselov, D. D. 2003, Nature, 421, 507
Kovács, G., Zucker, S., & Mazeh, T. 2002, A&A, 391, 369
Kovács, G., Bakos, G. Á., & Noyes, R. W. 2005, MNRAS, 356, 557
Johns-Krull, C. M., et al. 2008, ApJ, 677, 657
Latham, D. W. 1992, in IAU Coll. 135, Complementary Approaches to Double and Multiple Star Research, ASP Conf. Ser. 32, eds. H. A. McAlister & W. I. Hartkopf (San Francisco: ASP), 110
Liu, X., Burrows, A., & Ibgui, L.2008, astroph/0805.1733
Mandel, K., & Agol, E. 2002, ApJ, 580, L171
Mandushev, G. et al. 2005, ApJ, 621, 1061
Marcy, G. W., & Butler, R. P. 1992, PASP, 104, 270
McCullough, P. R., Stys, J. E., Valenti, J. A., Fleming, S. W., Janes, K. A., & Heasley, J. N. 2005, PASP, 117, 783
Pál, A., & Bakos, G. Á. 2006, PASP, 118, 1474
Pál, A. et al. 2008a, ApJ, 680, 1450
Pál, A., Bakos, G. Á., Noyes, R. W. & Torres, G. 2008c, to be appear in the proceedings of IAU Symp. 253 "Transiting Planets", ed. by F. Pont, astro-ph/0807.1530
Pollacco, D. L., et al. 2006, PASP, 118, 1407
Pont, F., Bouchy, F., Queloz, D., Santos, N. C., Melo, C., Mayor, M., & Udry, S. 2004, A&A, 426, L15
Queloz, D. et al. 2001, A&A, 379, 279
Sato, B., et al. 2005, ApJ, 633, 465
Southworth, J., Wheatley, P. J., & Sams, G. 2007, MNRAS, 379, 11
Sozzetti, A. et al. 2007, ApJ, 664, 1190
Torres, G., Boden, A. F., Latham, D. W., Pan, M. & Stefanik, R. P. 2002, AJ, 124, 1716
Torres, G., Konacki, M., Sasselov, D. D., & Jha, S. 2005, ApJ, 619, 558
Torres, G. et al. 2007, ApJ, 666, 121
Torres, G., Winn, J. N., Holman, M. J. 2008, ApJ, 677, 1324
Udalski, A., et al. 2002, Acta Astronomica, 52, 1
Udalski, A., et al. 2008, A&A, 482, 299
Valenti, J. A., & Piskunov, N. 1996, A&AS, 118, 595
Vogt, S. S. et al. 1994, Proc. SPIE, 2198, 362
Yi, S. K. et al. 2001, ApJS, 136, 417